Effect of size and shape on the excitonic stimulated emission process in ZnO microstructures

Matsuzaki, Ryosuke

Uchino, Takashi

Effect of size and shape on the excitonic stimulated emission process in ZnO microstructures

Ryosuke Matsuzaki, and Takashi Uchino

Citation: Journal of Applied Physics **124**, 063103 (2018); doi: 10.1063/1.5039790
View online: https://doi.org/10.1063/1.5039790
View Table of Contents: http://aip.scitation.org/toc/jap/124/6
Published by the American Institute of Physics

Effect of size and shape on the excitonic stimulated emission process in ZnO microstructures

Ryosuke Matsuzaki and Takashi Uchino[a)]
Department of Chemistry, Graduate School of Science, Kobe University, Nada, Kobe 657-8501, Japan

(Received 11 May 2018; accepted 24 July 2018; published online 9 August 2018)

There has been some (partly controversial) discussion about the role of excitons in room-temperature laser emission of ZnO. Recently, we have demonstrated from temperature and excitation-density-dependent photoluminescence measurements on a ZnO film consisting of well crystallized micrometer-sized grains that the mechanism of optical gain at temperatures below ~150 K is the exciton-exciton (ex-ex) scattering, whereas at temperatures from ~150 K to room temperature, the gain results from the exciton-electron (ex-el) scattering without any contribution from electron-hole plasma lasing [R. Matsuzaki *et al.*, Phys. Rev. B **96**, 125306 (2017)]. However, the mechanism of optical feedback inside these ZnO microstructures is not fully understood. In this work, we investigate the emission properties of various ZnO microcrystals with different size and shape in the temperature region from 3 to 300 K using a nanosecond pulsed laser as an excitation source. We found that room temperature stimulated emission is observed only from the sphere-like ZnO particles with the size of a few micrometers in diameter. We also found the temperature-induced transition between ex-ex and ex-el scattering processes at a temperature of ~150 K, similar to the case of the ZnO film consisting of micrometer-sized grains reported previously. The close similarity observed between the two different types of ZnO microstructures allows us to deduce that the temperature-dependent excitonic stimulated emission characteristics are common in micrometer-sized ZnO crystals with a low-loss feedback mechanism. *Published by AIP Publishing.*
https://doi.org/10.1063/1.5039790

I. INTRODUCTION

Since the discovery of optically pumped lasing from polycrystalline ZnO,[1,2] epitaxially grown ZnO thin films,[3,4] and well-aligned ZnO nanowires[5] at room temperature, a great number of studies have been carried out to investigate the underlying mechanism responsible for the lasing behavior.[1–22] In particular, much attention has been devoted to Fabry-Perot nanowire laser[5,9–11] and nanoparticle-based random laser.[1,2,20–22] It has then been demonstrated that the lasing characteristics such as lasing threshold, lasing wavelength, and lasing modes are dependent not only on the crystallinity but also on the size, shape, and morphology of ZnO.[6–10,20]

Nanoparticle-based random laser is realized by recurring multiple scattering events of light in aggregated ZnO particles with sizes of several hundreds of nanometers.[1,2,22] In these ZnO nanostructures, lasing spikes, i.e., discrete emission peaks with a linewidth of less than ~1 nm, are observed at pumping intensities over the threshold excitation for lasing. It has also been demonstrated that both localized and extended modes contribute to the generation of the lasing spikes from ZnO nanostructures.[23] This indicates that random lasing occurs not only in strongly scattering systems but also in weakly scattering ones[24–26] although the true physical origin of the narrow random lasing lines is still being debated.[27]

However, when the size of ZnO particles becomes larger than several micrometers, such narrow lasing spikes are not normally observed. It is hence probable that the conditions for realizing localized and/or extended modes are not reached in powders of micrometer-sized ZnO particles. Notwithstanding the absence of random lasing spikes, we can still expect the realization of feedback in the micrometer-sized ZnO particles. The relevant feedback in the ZnO microcrystals will not be coherent but can be used merely to return part of the energy or photons to the starting point, leading to energy or intensity feedback. This type of random laser is referred to as random laser with incoherent feedback,[22,28] in contrast to the case of nanoparticle-based random laser with coherent feedback.[22,26]

Recently, we[29] have demonstrated that the incoherent-feedback random lasing is likely to be realized in a film consisting of well-crystallized micrometer-sized ZnO grains. It should be stressed that room-temperature excitonic lasing is observed from the film of micrometer-sized grains without showing any symptoms of electron-hole plasma (EHP) emission. We[29] have also found that the temperature-induced transition from the exciton-exciton (ex-ex) scattering to the exciton-electron (ex-el) scattering occurs at temperatures near ~150 K; the ex-el process continues to exist with further increasing temperature up to room temperature. The long carrier diffusion length and the low optical loss nature of the micrometer-thick ZnO films presumably play a key role in showing purely excitonic lasing at room temperature. In such micrometer-sized ZnO crystals, the concentration gradients of the photogenerated carriers created at the near surface will push them deeper into the sample,[30] rapidly reducing their concentration below the Mott density even

a)Electronic mail: uchino@kobe-u.ac.jp

under highly excited conditions to allow pure excitonic lasing. These results will shed light on the nature of the room-temperature excitonic lasing in ZnO because its true physical origin, which was initially attributed to exciton-exciton (ex-ex) scattering process,[4,13] is still a matter of discussion.[17–19]

Although the ex-el scattering has been shown to be the principal gain process in ZnO microcrystals at room-temperature, the mechanism of the optical (mirrorless) feedback in these microstructured systems is still not well understood. To investigate this further, we perform systematic photoluminescence (PL) measurements of various ZnO microstructures with different size and shape. We show that excitonic lasing is observed exclusively from the sphere-like ZnO particles with a size larger than a few micrometers. Also, the temperature-induced transition between the ex-ex and ex-el processes has been shown to occur at ∼150 K in these sphere-like ZnO microparticles, in agreement with the results observed from the ZnO film of micrometer-sized grains.[29]

II. EXPERIMENTAL PROCEDURES

We prepared micrometer-sized ZnO particles by thermal decomposition of zinc acetate dihydrate,[31,32] which is a simple but effective method to obtain variously sized and shaped ZnO particles. We first pre-annealed ∼2.6 g of reagent grade zinc acetate dihydrate (Sigma-Aldrich, purity ≥98%), which was placed in an aluminum crucible covered with an alumina lid, in an electric furnace at 300 °C for 12 h in air atmosphere. The resulting materials were washed with distilled water and dried in an oven at 90 °C for 12 h. The dried samples were then post-annealed at 800 – 1100 °C for 3 h in air. The resulting samples were stored in a desiccator for later characterization. Powder X-ray diffraction (XRD) patterns were obtained with a diffractometer (Rigaku, SmartLab) using Cu Kα radiation. Scanning electron microscopy (SEM) was conducted with a scanning electron microscope (JEOL, JSM-5510). PL measurements were carried out with a gated image intensified charge-coupled device (Princeton Instruments, PI-MAX:1024RB) and 1800 or 300 lines/mm grating by using the third harmonic (355 nm) of a Q-switched Nd:yttrium aluminum garnet (YAG) laser (Spectra Physics, INDI 40, pulse width ∼10 ns, repetition rate 10 Hz) as an excitation source. During the PL measurements, the laser pulse was irradiated onto a quartz sample holder containing ZnO powder without focusing the laser beam (beam spot size of ∼7 mm), and the emission signal from the front surface was monitored. The sample temperature was controlled in an optical cryostat system in the temperature region from 3 to 300 K.

III. RESULTS

Figure 1 shows the XRD patterns and SEM images of the samples post-annealed at different temperatures from 800 to 1100 °C. Although all the samples have the hexagonal wurtzite structure of ZnO [Fig. 1(a)], the crystalline morphology varies from deformed rod-like (∼100 nm in diameter, ∼2 μm in length) to irregular spherical shapes (typical size ∼2 – 3 μm in diameter) with increasing annealing

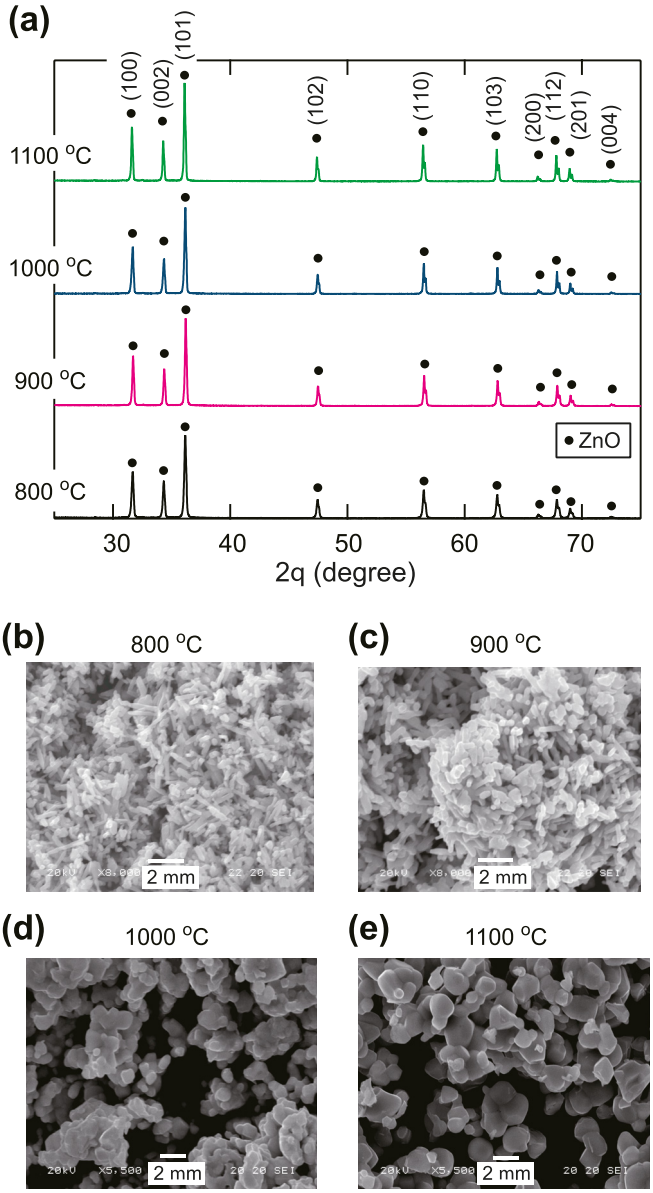

FIG. 1. (a) XRD patterns of the ZnO samples prepared at different temperatures. (b)-(d) SEM images of the ZnO samples prepared at (b) 800 °C, (c) 900 °C, (d) 1000 °C, and (e) 1100 °C.

temperature, as shown in the SEM images in panels (b) to (e) in Fig. 1.

Room-temperature PL spectra of these micrometer-sized ZnO crystals for increasing optical excitation are shown in Fig. 2 in a semi-log plot. The near-band edge (NBE) emission of the 800 °C sample exhibits a broad spectral feature under the excitation fluence I ranging from 0.3 to 52 mJ/cm^2 [Fig. 2(a)]. This broad NBE emission stems from the superimposition of the thermally broadened free exciton (FX) recombination and its longitudinal-optical (LO) phonon replica.[33,34] Note also that this broad emission feature is observed from all the samples employed in this work [Figs. 2(b)–2(d)], indicating that this excitonic band is due to spontaneous emission and therefore occurs irrespective of the shape and size of the particles. Also, the PL spectra of the 800 °C sample shows an almost linear increase in intensity and bandwidth with increasing I up to ∼20 mJ/cm^2, followed

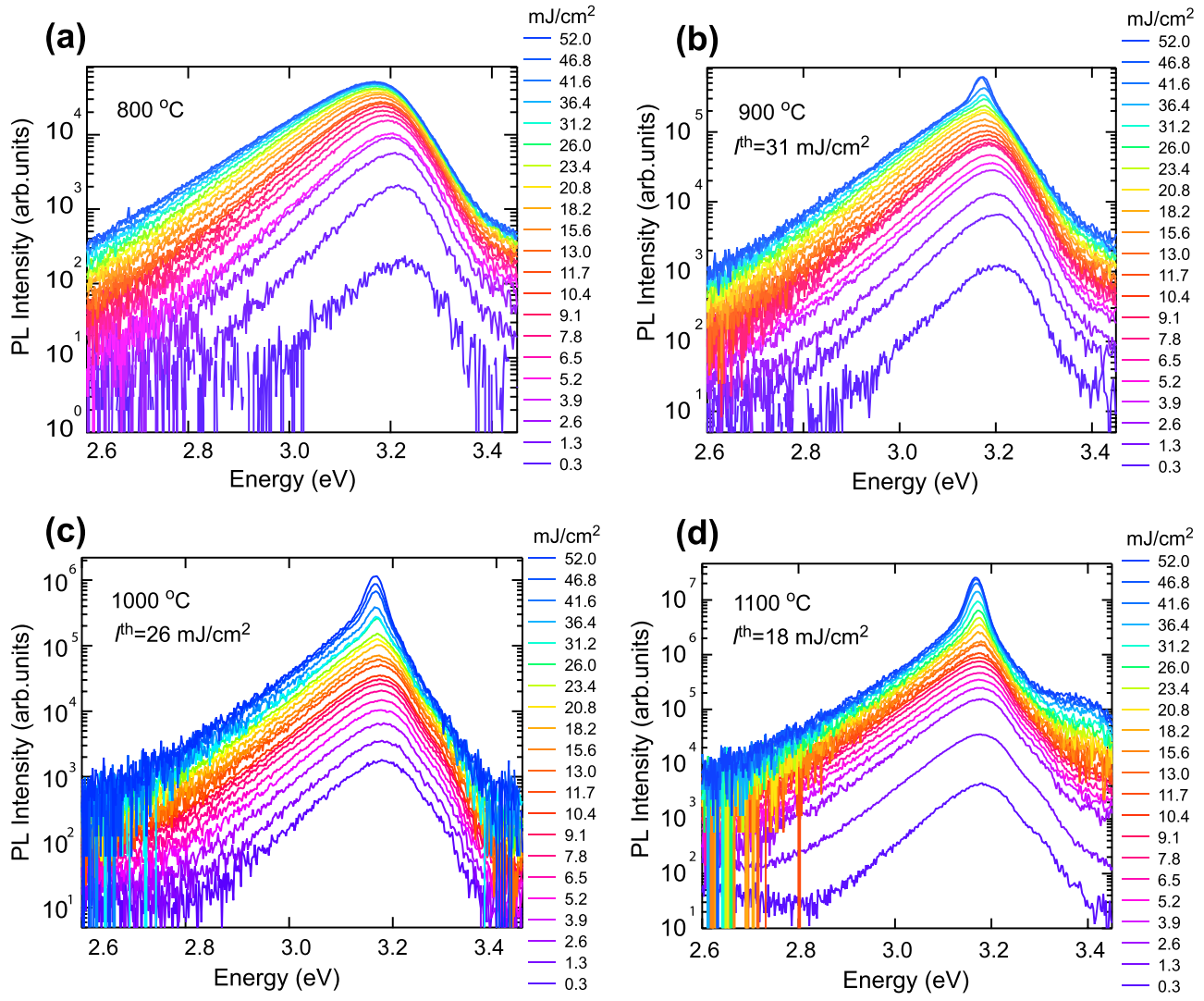

FIG. 2. Excitation fluence dependence of the room-temperature PL spectra of the ZnO samples prepared at (a) 800 °C, (b) 900 °C, (c) 1000 °C, and (d) 1100 °C. In (b) and (c), the threshold fluence for spectral narrowing (Ith) is shown.

by saturation at higher excitation fluences [Fig. 3(a)]. This result is consistent with the spontaneous emission scenario. However, the NBE emission of the samples prepared at temperatures higher than 900 °C exhibits spectral narrowing under highly excited conditions [Figs. 2(b)–2(d)], implying the occurrence of laser action. Indeed, as shown in Fig. 3(b), the spectral narrowing of the 1100 °C annealed sample is accompanied by a nonlinear increase in the integrated emission intensity with increasing I [Figs. 2(b)–2(d)], thus supporting the lasing interpretation. The lasing threshold (Ith) can be defined as the pumping fluence at which the spectral narrowing initially sets in. We found that Ith decreases with increasing post-annealing temperature, i.e., the Ith values of the 900, 1000, and 1100 °C annealed samples are 31, 26, and 18 mJ/cm^2, respectively. Note, however, that the present lasing is most likely due to the random lasing

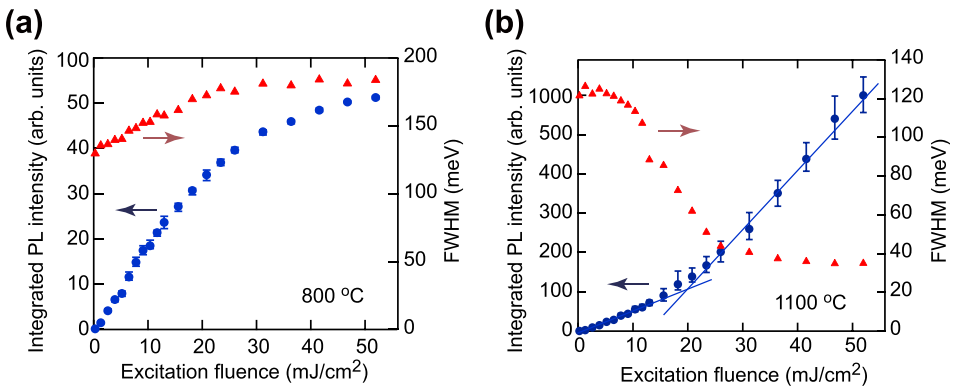

FIG. 3. The excitation fluence dependence of the full width at half maximum (FWHM, right axis) and the spectrally integrated PL intensity (left axis) of the ZnO samples prepared at (a) 800 °C and (b) 1100 °C.

with incoherent feedback since no modal emission is observed, as will be discussed in more detail in Sec. IV. These observations suggest that ZnO particles with larger spherical shapes preferentially contribute to the narrowing behavior. It should also be worth mentioning that as shown in Figs. 2(b)–2(d), the peak energy and width of the observed lasing spectra are almost constant as I increases from ~10 to ~50 mJ/cm^2. This indicates that bandgap renormalization due to many-body effects in an EHP[35] does not occur in the sample under the present excitation condition. These results are quite similar to those reported previously for the ZnO film consisting of micrometer-sized grains.[29]

To further investigate the lasing characteristics of the micrometer-sized ZnO particles, we next carried out low-temperature PL measurements for the 1100 °C sample. Figure 4 shows the excitation-fluence-dependent PL spectra measured at 3 K. The PL spectrum obtained under the lowest excitation fluence ($I_{exc} = 0.1$ mJ/cm^2) shows several emission lines at 3.360, ~3.31, ~3.29, and ~3.22 eV. The peak at 3.360 eV is attributed to a donor bound exciton emission (D^0X),[36,37] and the two lower energy peaks at ~3.29 and ~3.22 eV to its first and second longitudinal optical (LO) phonon replicas (D^0X-LO and D^0X-2LO), respectively.[37] The ~3.31-eV band is likely to result from the stacking fault related transition[38,39] and/or the first LO phonon replica of the free exciton (FX-LO).[39,40] As the excitation fluence increases, one finds that two additional peaks grow on the lower energy side of the D^0X band. One is the peak at 3.353 eV, which can be recognized in the PL spectra obtained at $I = 0.3$ mJ/cm^2 or higher. This emission is tentatively attributed to the donor-bound biexciton (D^0M).[41,42] When I exceeds ~4 mJ/cm^2, the other peak develops in the 3.32–3.33 eV region [see the pink-colored area in Fig. 4(a)]. This peak dominates the entire spectrum for $I \gtrsim 10$ mJ/cm^2 and shows a slight red shift with a further increase in I. The integrated emission intensity shows a nonlinear increase with increasing excitation fluence with an excitation threshold of ~7 mJ/cm^2 [Fig. 4(b)]. This newly developed peak can be attributed to the stimulated emission induced by ex-ex scattering, in which one exciton recombines radiatively, while the other is scattered into a higher state ($n = 2,3, \ldots\infty$). The emission maxima of the ex-ex process can be given by[43]

$$\hbar\omega_{max}^{ex-ex}(T) = E_{ex}(T) - E_b\left(1 - \frac{1}{n^2}\right) - \frac{3}{2}k_BT, \qquad (1)$$

where $E_{ex}(T)$ is the free exciton transition energy at a temperature T, E_b is the binding energy of the exciton (60 meV), and k_B is the Boltzmann constant. When we assume that $E_{ex}(T) = 3.377$ eV at 3 K,[33] Eq. (1) yields the emission maxima at 3.332 and 3.317 eV for $n = 2$ and ∞, respectively. These values are in good agreement with the higher (3.330 eV) and lower (3.316 eV) limits of the pink-colored region in Fig. 4(a).

We next measured the temperature dependent PL spectra under the constant excitation fluence of $I = 36$ mJ/cm^2, which is sufficient enough to induce stimulated emission both at low and room temperatures. Under this excitation condition, as shown in Fig. 5(a), a single sharp emission band is observed over the whole temperature range investigated (3–300 K). Figure 5(b) shows the peak energy of this emission band as a function of temperature. In Fig. 5(b), we also show the temperature dependence of the free-exciton transition energy $E_{ex}(T)$ reported for bulk ZnO[33] and the ex-ex scattering energies for $n = 2$ and ∞ predicted from Eq. (1). One sees from Fig. 5(b) that in the temperature range from 3 to ~150 K, the observed peak energy lies within the energy range predicted for the ex-ex scattering process. At temperatures above ~150 K, however, the observed peak energy shows a substantial deviation from the energy range of the ex-ex scattering, implying the onset of an alternative emission process. We found that similar to the case of the ZnO film of micrometer-sized grains,[29] the temperature dependence of the expected alternative process is well described by that of the exciton-electron (ex-el) scattering process, which is given by[43–45]

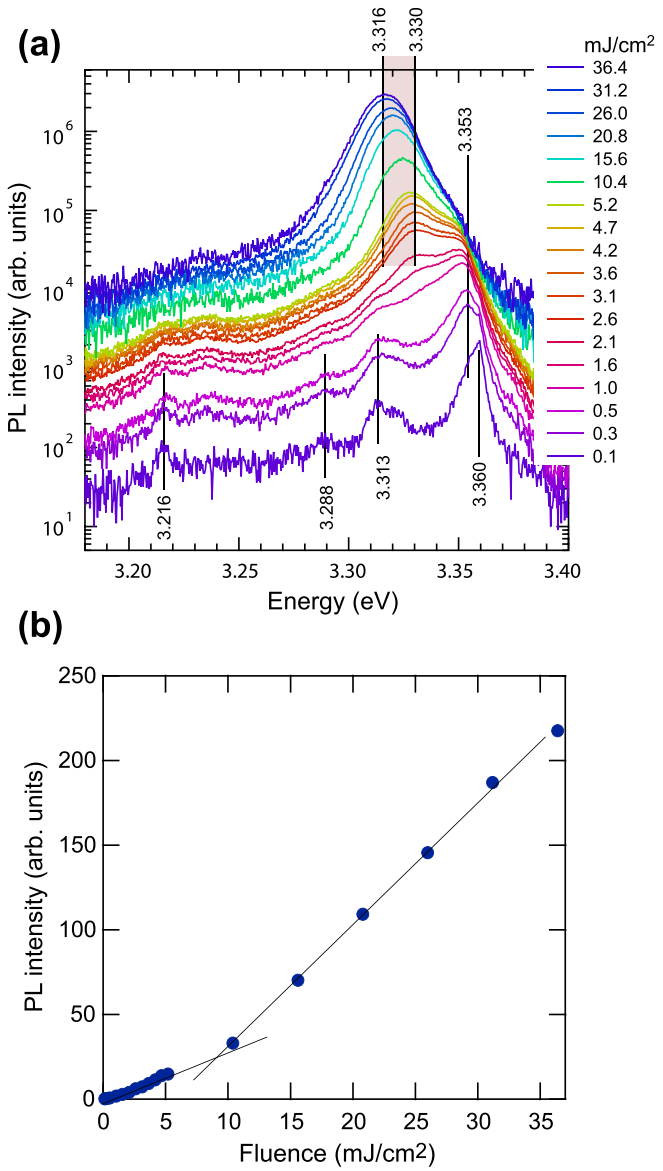

FIG. 4. PL characteristics of the 1100 °C annealed sample measured at 3 K. (a) Changes in the PL spectra with increasing excitation fluence from 0.1 to 36.4 mJ/cm^2. (b) Excitation fluence dependence of the spectrally integrated PL intensity.

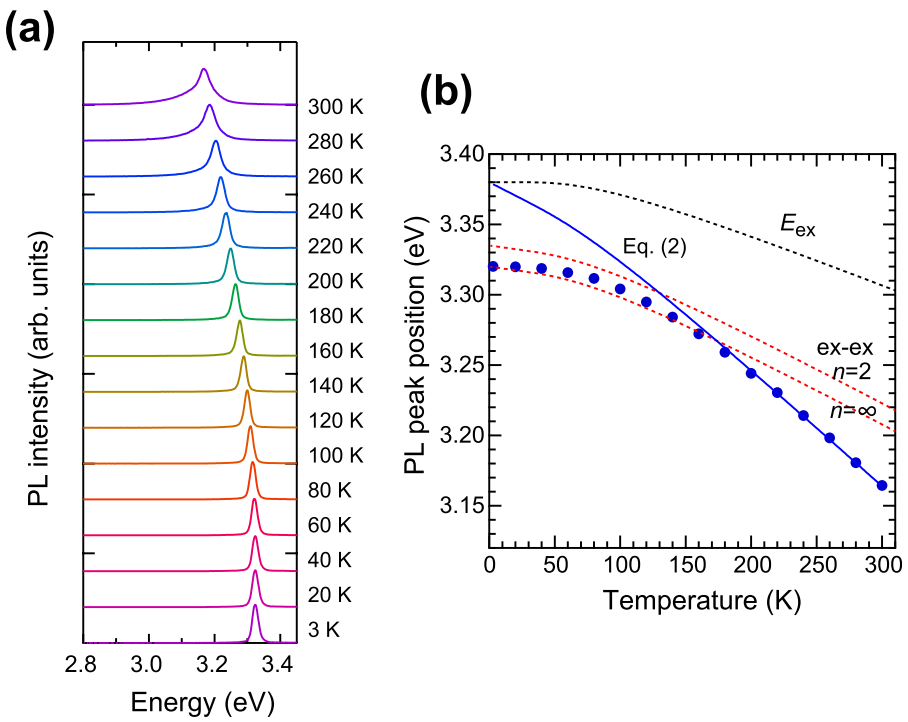

FIG. 5. (a) Changes in the lasing spectra of the 1100 °C annealed sample with increasing temperature from 3 to 300 K measured under a constant excitation fluence of 36 mJ/cm^2. The peak intensities are normalized among all spectra, which are displaced vertically for clarity. (b) The peak energy of the lasing spectra shown in (a) (filled circles) as a function of temperature. The solid (blue) line shows a least-squares fit of the data in the 160–300 K region to Eq. (2). The free-exciton transition energy (E_{ex}) reported in Ref. 33 and the emission maxima of the ex-ex process for $n=2$ and $n=\infty$ calculated from Eq. (1) are also shown.

$$\hbar\omega_{\max}^{\text{ex-el}}(T) = E_{ex}(T) - \gamma k_B T, \tag{2}$$

where γ is a constant related to the ratio of exciton effective mass over electron effective mass. The fitting with Eq. (2) was performed for the data points in the 160–300 K range, and the result of fitting is shown in Fig. 5(b) as a solid (blue) line. The best fitted value of γ is 5.5, which is slightly smaller than the one obtained for the ZnO film of micrometer-sized grains (γ =6.1)[29] but is still in reasonable agreement with the predicted value of γ =∼7.[43,44]

IV. DISCUSSION

We have shown that the ZnO aggregates obtained by post-annealing at 800 °C did not show any lasing action [see Fig. 2(a)]. This is probably due to their highly deformed and ill-crystalized structures, in which the optical loss and surface recombination of these small grains are too large to exhibit a practical laser action. As the post-annealing temperature increases, the ZnO aggregated particles tend to become large and spherical although still deformed. Accordingly, one can recognize the lasing behavior, i.e., the appreciable spectral narrowing and nonlinear intensity enhancement of the luminescence, for the samples obtained by post-annealing at temperatures above 900 °C [see Figs. 2(a)–2(c)]. It can hence safely be assumed that the low-loss feedback condition is achieved in the large spherical ZnO grains. Note, however, that the spatial resonances for the electromagnetic field are likely to be absent because light will not necessarily return to its original position after one round trip in these deformed particles. We hence consider that the feedback is non-resonant and is used only to return part of the photon energy to the gain medium, resulting only in incoherent energy feedback.[22,24] Indeed, we did not observe a spiky feature, which is an indication of coherent feedback,[22,26] and it is absent in the present lasing spectra. In such an incoherent energy feedback system, the mean frequency of laser emission does not depend on the dimensions of the gain medium but is determined only by the center frequency of the amplification line.[46] This can explain the observation shown in panels (b), (c), and (d) in Fig. 2 that the present ZnO microparticles prepared after different post-annealing temperatures exhibit basically the same lasing peak at 3.17 eV at room temperature.

It should also be worth mentioning that the excitonic lasing behavior of the present ZnO microparticles is quite similar to that of the ZnO film of micrometer-sized grains.[29] Both the samples not only exhibit a transition from ex-ex to ex-el processes at ∼150 K but also demonstrate no signs of EHP emissions under the present excitation conditions (≲50 mJ/cm^2). The only apparent difference between the two samples is the excitonic lasing threshold I_{EX}^{th}; the I_{EX}^{th} values for the film and the particle samples are ∼2 mJ/cm^2 (or ∼200 kW/cm^2) and ∼20 mJ/cm^2 (or ∼2 MW/cm^2), respectively, at room temperature. We suggest that the higher threshold of the particle samples results from the low efficiency of the energy feedback because of their irregular shape and high optical loss. However, the absence of the EHP emission implies that that the density of electron-hole pairs n_p is still below the Mott density at I_{EX}^{th} even for the present particle samples. It is hence interesting to estimate the n_p values at I_{EX}^{th} for these samples. When the sample size d is comparable to or larger than the diffusion length l_D (∼3 μm) of the excited carriers, which is the case for the present micrometer-sized ZnO crystals, n_p can be estimated by[17]

$$n_p = \frac{P\tau}{\hbar\omega l_D}, \tag{3}$$

where P and $\hbar\omega$ are the excitation power (in W/cm^2) and the photon energy (in J) of the light source, respectively, and τ is the decay time of the stimulated emission (4 ps[29]). As

mentioned in Ref. 29, n_p of the ZnO film of micrometer-sized grains at the lasing threshold ($P \approx 200\,\mathrm{kW/cm^2}$) is estimated to be $\sim 5 \times 10^{15}\,\mathrm{cm^{-3}}$, which is two or three orders of magnitude lower than the reported value of the Mott density ($\sim 10^{18}\,\mathrm{cm^{-3}}$).[11,17,47] On the other hand, n_p of the micrometer-sized ZnO particles at the threshold ($P \approx 2\,\mathrm{MW/cm^2}$) is calculated to be $\sim 5 \times 10^{16}\,\mathrm{cm^{-3}}$. The resulting electron-hole density is still at least an order of magnitude lower than the Mott density. Thus, the evaluation of n_p allows us to confirm that the room-temperature lasing of the micrometer-sized ZnO particles observed under the present excitation condition is of excitonic origin. It is hence most likely that when the appropriate low-loss feedback condition is satisfied, micrometer-sized ZnO structures can exhibit common excitonic lasing behaviors in a wide temperature region, including room temperature.

V. CONCLUSIONS

We have carried out systematic PL measurements of the differently sized/shaped ZnO particles. The lasing threshold, which corresponds to a condition in which the photon loss rate is balanced by the photon generation rate in the amplifying region, decreases as the particles grow into sphere-like structures with the size of a few micrometers. It is most likely that the incoherent energy feedback is responsible for the observed lasing action. As for these sphere-like particles, the gain mechanism is changed from the ex-ex scattering (below $\sim 150\,\mathrm{K}$) to the ex-el scattering (above $\sim 150\,\mathrm{K}$) with increasing temperatures. The density of electron-hole pairs at the room-temperature lasing threshold is an order of magnitude lower than the Mott density, confirming that the EHP process is not responsible for the observed room-temperature lasing. These results are basically in agreement with those of the ZnO film consisting of well crystallized micrometer-sized grains[29] although its preparation method and apparent morphology are quite different from those of the ZnO particles used in the study. Thus, it can be concluded that the room-temperature excitonic stimulated emission and its temperature induced transition are commonly observed from micrometer-sized ZnO structures as long as the low-loss feedback condition is achieved during optical pumping.

[1] H. Cao, Y. G. Zhao, S. T. Ho, E. W. Seelig, Q. H. Wang, and R. P. H. Chang, Phys. Rev. Lett. **82**, 2278 (1999).
[2] H. Cao, J. Y. Xu, D. Z. Zhang, S.-H. Chang, S. T. Ho, E. W. Seeling, X. Liu, and R. P. H. Chang, Phys. Rev. Lett. **84**, 5584 (2000).
[3] D. M. Bagnall, Y. F. Chen, Z. Zhu, T. Yao, S. Koyama, M. Y. Shen, and T. Goto, Appl. Phys. Lett. **70**, 2230 (1997).
[4] P. Zu, Z. K. Tang, G. K. L. Wong, M. Kawasaki, A. Ohtomo, H. Koinuma, and Y. Segawa, Solid State Commun. **103**, 459 (1997).
[5] M. H. Huang, S. Mao, H. Feick, H. Yan, Y. Wu, H. Kind, E. Weber, R. Russo, and P. Yang, Science **292**, 1897 (2001).
[6] Ü. Özgür, Ya. I. Alivov, C. Liu, A. Teke, M. A. Reshchikov, S. Dogan, V. Avrutin, S.-J. Cho, and H. Morkoç, J. Appl. Phys. **98**, 041301 (2005).
[7] A. B. Djurišić and Y. H. Leung, Small **2**, 944–961 (2006).
[8] C. Klingshirn, J. Fallert, H. Zhou, J. Sartor, C. Thiele, F. Maier-Flaig, D. Schneider, and H. Kalt, Phys. Status Solidi B **247**, 1424 (2010).
[9] D. Vanmaekelbergh and L. K. van Vugt, Nanoscale **3**, 2783 (2011).
[10] M. Zimmler, F. Capasso, S. Müller, and C. Ronning, Semicond. Sci. Technol. **25**, 024001 (2010).
[11] M. A. M. Versteegh, D. Vanmaekelbergh, and J. I. Dijkhuis, Phys. Rev. Lett. **108**, 157402 (2012).
[12] C. Xu, J. Dai, G. Zhu, G. Zhu, Y. Lin, J. Li, and Z. Shi, Laser Photonics Rev. **8**, 469 (2014).
[13] D. M. Bagnall, Y. F. Chen, Z. Zhu, T. Yao, M. Y. Shen, and T. Goto, Appl. Phys. Lett. **73**, 1038 (1998).
[14] Ü. Özgür, A. Teke, C. Liu, S. J. Cho, H. Morkoç, and H. O. Everitt, Appl. Phys. Lett. **84**, 3223 (2004).
[15] A.-S. Gadallah, K. Nomenyo, C. Couteau, D. J. Rogers, and G. Lérondel, Appl. Phys. Lett. **102**, 171105 (2013).
[16] Z. K. Tang, M. Kawasaki, A. Ohtomo, H. Koinuma, and Y. Segawa, J. Cryst. Growth **287**, 169 (2006).
[17] C. Klingshirn, R. Hauschild, J. Fallert, and H. Kalt, Phys. Rev. B **75**, 115203 (2007).
[18] C. Klingshirn, J. Fallert, O. Gogolin, M. Wissinger, R. Hauschild, M. Hauser, H. Kalt, and H. Zhou, J. Lumin. **128**, 792 (2008).
[19] D. M. Bagnall, in *Zinc Oxide Materials for Electronic and Optoelectronic Devices and Applications*, edited by C. W. Litton, D. C. Reynolds, and T. C. Collins (Wiley, Chichester, 2011), pp. 265–284.
[20] J. Fallert, R. J. B. Dietz, H. Hauser, F. Stelzl, C. Klingshirn, and H. Kalt, J. Lumin. **129**, 1685 (2009).
[21] T. Nakamura, K. Firdaus, and S. Adachi, Phys. Rev. B **86**, 205103 (2012).
[22] H. Cao, in *Progress in Optics*, edited by E. Wolf (Elsevier, Amsterdam, 2003), Vol **45**, pp. 317–370.
[23] J. Fallert, R. J. B. Dietz, J. Sartor, D. Schneider, C. Klingshirn, and H. Kalt, Nat. Photonics **3**, 279 (2009).
[24] S. Mujumdar, M. Ricci, R. Torre, and D. S. Wiersma, Phys. Rev. Lett. **93**, 053903 (2004).
[25] C. Vanneste, P. Sebbah, and H. Cao, Phys. Rev. Lett. **98**, 143902 (2007).
[26] D. S. Wiersma, Nat. Phys. **4**, 359 (2008).
[27] D. S. Wiersma, Nat. Photonics **7**, 188 (2013).
[28] F. Luan, B. Gu, A. S. L. Gomes, K.-T. Yong, S. Wen, and P. N. Prasad, Nano Today **10**, 168 (2015).
[29] R. Matsuzaki, H. Soma, K. Fukuoka, K. Kodama, A. Asahara, T. Suemoto, Y. Adachi, and T. Uchino, Phys. Rev. B **96**, 125306 (2017).
[30] G. Tobin, E. McGlynn, M. O. Henry, J.-P. Mosnier, E. de Posada, and J. G. Lunney, Appl. Phys. Lett. **88**, 071919 (2006).
[31] C.-C. Lin and Y.-Y. Li, Mater. Chem. Phys. **113**, 334 (2009).
[32] X. Zhang, J. Qin, Y. Xue, P. Yu, B. Zhang, L. Wang, and R. Liuc, Sci. Rep. **4**, 4596 (2014).
[33] L. Wang and N. C. Giles, J. Appl. Phys. **94**, 973 (2003).
[34] S. L. Chen, S. K. Lee, W. M. Chen, H. X. Dong, L. Sun, Z. H. Chen, and I. A. Buyanova, Appl. Phys. Lett. **96**, 033108 (2010).
[35] C. Klingshirn, *Semiconductor Optics*, 3rd ed. (Springer, Berlin, 2007).
[36] M. R. Wagner, G. Callsen, J. S. Reparaz, J.-H. Schulze, R. Kirste, M. Cobet, I. A. Ostapenko, S. Rodt, C. Nenstiel, M. Kaiser, A. Hoffmann, A. V. Rodina, M. R. Phillips, S. Lautenschläger, S. Eisermann, and B. K. Meyer, Phys. Rev. B **84**, 035313 (2011).
[37] A. Teke, Ü. Özgür, S. Doğan, X. Gu, H. Morkoç, B. Nemeth, J. Nause, and H. O. Everitt, Phys. Rev. B **70**, 195207 (2004).
[38] M. Schirra, R. Schneider, A. Reiser, G. M. Prinz, M. Feneberg, J. Biskupek, U. Kaiser, C. E. Krill, K. Thonke, and R. Sauer, Phys. Rev. B **77**, 125215 (2008).
[39] D. Tainoff, B. Masenelli, P. Mélinon, A. Belsky, G. Ledoux, D. Amans, C. Dujardin, N. Fedorov, and P. Martin, Phys. Rev. B **81**, 115304 (2010).
[40] L. Sun, H. He, and Z. Ye, Appl. Phys. A **115**, 879 (2014).
[41] A. Yamamoto, K. Miyajima, T. Goto, H. J. Ko, and T. Yao, J. Appl. Phys. **90**, 4973 (2001).
[42] A. Yamamoyo, K. Miyajima, T. Goto, H. J. Ko, and T. Yao, Phys. Status Solidi B **229**, 871 (2002).
[43] C. Klingshirn, Phys. Status Solidi B **71**, 547 (1975).
[44] B. Hönerlage, C. Klingshirn, and J. B. Grun, Phys. Status Solidi B **78**, 599 (1976).
[45] C. I. Yu, T. Goto, and M. Ueta, J. Phys. Soc. Jpn. **34**, 693 (1973).
[46] G. van Soest and A. Lagendijk, Phys. Rev. E **65**, 047601 (2002).
[47] A. Schleife, C. Rödl, F. Fuchs, K. Hannewald, and F. Bechstedt, Phys. Rev. Lett. **107**, 236405 (2011).